Article

Amantamide C, an Antitrypanosomal Linear Lipopeptide from a Marine *Okeania* sp. Cyanobacterium

Natsumi Watanabe, Ghulam Jeelani, Tomoyoshi Nozaki, and Arihiro Iwasaki*

Read Online

ACCESS | Metrics & More | Article Recommendations | Supporting Information

ABSTRACT: Amantamides are lipopeptides that act as selective CXC chemokine receptor 7 agonists and modulate spontaneous calcium oscillations in primary cultured neocortical neurons. We isolated a new analog of amantamides, amantamide C, from marine *Okeania* sp. cyanobacterium collected in Japan and established its structure based on NMR and MS/MS analyses, and degradation reactions. In addition, we evaluated the biological activity of amantamide C and revealed novel biological features of amantamide-type compounds.

Amantamide C

Anti-Trypanosomal activity

Okeania sp.
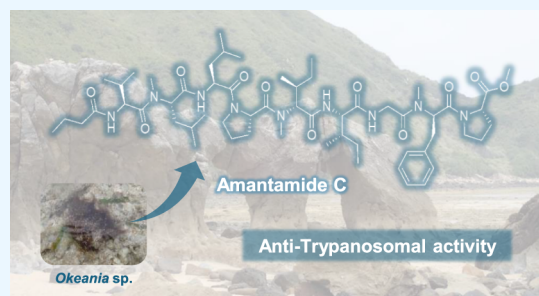
INTRODUCTION

Marine cyanobacteria have attracted considerable attention as prolific producers of secondary metabolites. One of the major groups of marine cyanobacterial metabolites is a linear lipopeptide possessing an $O-Me-_L-Pro-N-Me-_D-Phe$ substructure at the O−terminal, such as tasiamides A−E,[1] grassystatins,[2] izenamides,[3] and maedamide.[4] In 2018, Al-Awadhi et al. isolated other compounds in this group, brintonamides A−E,[5] from a marine cyanobacterium collected in Florida and characterized them as G protein-coupled receptor (GPCR) modulators. Inspired by this discovery, in 2019 Liang et al. isolated a lipopeptide in the same group, amantamide (**2**), and demonstrated that **2** is a selective agonist against CXC-chemokine receptor 7 (CXCR7) among 168 GPCR.[6] CXCR7, also known as atypical chemokine receptor 3 (ACKR3), has been recently recognized as a novel target for treatment of advanced prostate cancer because CXCR7 appears to play an essential role in regulating cancer progression.[7] Furthermore, in 2022 Li et al. isolated a new analog of amantamide, amantamide B (**3**), from *Oscillatoria* sp. cyanobacterium collected in the South China Sea and reported that amantamides (**2** and **3**) modulate spontaneous calcium oscillations of primary cultured neocortical neurons.[8] Their discovery indicated that the biological activity of **2** and **3** is related to neuronal excitation and/or potential activity on Ca^{2+} signaling, but detailed relations to agonistic activities against CXCR7 remained unknown.

Herein, we isolated another analog of amantamides, amantamide C (**1**), from *Okeania* sp. marine cyanobacterium collected in Japan and revealed its biological features, which have not been reported for **2** or **3**.

amantamide C (**1**) : R₁ = Me, R₂ = H
amantamide   (**2**) : R₁ = H, R₂ = H
amantamide B (**3**) : R₁ = H, R₂ = Me
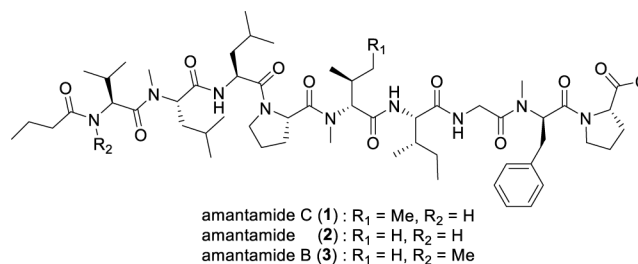
RESULTS AND DISCUSSION

The cyanobacteria sample (810 g, wet weight) was collected on the coast of Tonaki Island in Japan, near an eyeglasses-shaped rock locally known as "Fugimi". It was classified into *Okeania* sp. by phylogenetic analysis based on the 16S rRNA genes. The samples were extracted with methanol (MeOH), filtered, and concentrated. The residue was partitioned between ethyl acetate (EtOAc) and water. The organic layer was partitioned using hexane and 90% aqueous MeOH. The material obtained from the 90% aqueous MeOH portion was fractionated by reversed-phase open column chromatography and repeated reversed-phase HPLC to give a fraction that contained amantamide C (**1**, please see the Experimental Section for details). This fraction induced spindle-like morphological change to HeLa cells (Figure S1). As a result of further HPLC purification of this fraction directed by this
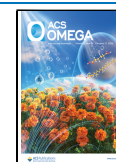
Table 1. NMR Data for Amantamide C (1) in CD$_3$OD[a]

residue	position	δ_C[b]	δ_H[c] (J in Hz)	COSY	selected TOCSY	selected HMBC (H→C)	selected NOESY
O-Me-Pro	1	174.0, C					
	2	60.7, CH	4.38, dd (8.5, 6.0)	3a, 3b	3a, 3b, 4a, 4b, 5		
	3a	30.0, CH$_2$	2.22, m	2, 3b	2, 3b, 4a, 4b, 5		
	3b		1.86, m	2, 3a	2, 3a, 4a, 4b, 5		
	4a	26.1[e], CH$_2$	1.95, m	5, 4b	2, 3a, 3b, 4b, 5		
	4b		1.86, m	5, 4a	2, 3a, 3b, 4a, 5		
	5	48.5, CH$_2$	3.41, m	4a, 4b	2, 3a, 3b, 4a, 4b		N-Me-Phe-2
	6	52.6, CH$_3$	3.71, s			1	
N-Me-Phe	1	170.3, C					
	2	57.7, CH	5.55, t (7.4)	3a, 3b		1	O-Me-Pro-5
	3a	35.6, CH$_2$	3.15, m	2, 3b		4, 5/9	
	3b		2.75, dd (13.6, 7.4)	2, 3a		4, 5/9	
	4	138.9, C					
	5/9	130.5, CH	7.19, m			6/8	
	6/8	129.3, CH	7.19, m	7		5/9	
	7	127.4, CH	7.14, m	6/8			
	10	30.7, CH$_3$	3.05, s			2, Gly-1	Gly-2a, Gly-2b
Gly	1	170.1, C					
	2a	42.1, CH$_2$	4.35, d (16.9)	2b		1	N-Me-Phe-10
	2b		3.88, d (16.9)	2a		1	N-Me-Phe-10
	NH[d]		7.56, dd (6.2, 4.0)	2a, 2b			
Ile	1	173.8, C					
	2	59.7, CH	4.28, d (6.5)	3	3, 4b, 5, 6	1	
	3	37.5, CH	1.95, m	2, 4b, 6	2, 4a, 4b, 5		
	4a	26.0[e], CH$_2$	1.48, m	4b	3, 4b, 5, 6		
	4b		1.20, m	3, 4a, 5	2, 3, 4a, 5, 6		
	5	11.3, CH$_3$	0.91, m	4b	2, 3, 4a, 4b, 6		
	6	16.2, CH$_3$	0.96, m	3	2, 3, 4a, 4b, 5		
	NH[d]		7.75, d (8.0)	2		N-Me-Ile-1	
N-Me-Ile	1	171.5, C					
	2	62.1, CH	4.77, d (10.8)	3	3, 4a, 4b, 5, 6	1	7
	3	33.2, CH	2.12, m	2	2, 5, 6		
	4a	27.4, CH$_2$	1.11, m	4b, 5	2, 4b, 5, 6		
	4b		1.45, m	4a, 5	2, 4a, 5, 6		
	5	11.6, CH$_3$	0.94, m	4a, 4b	3, 4a, 4b		
	6	14.6, CH$_3$	0.81, d (6.5)	3	3, 4a, 4b		
	7	31.5, CH$_3$	3.01, s			2, Pro-1	2, Pro-2
Pro	1	175.08[e], C					
	2	58.9, CH	4.71, dd (8.2, 5.7)	3a, 3b	3a, 3b, 4a, 4b, 5a, 5b		N-Me-Ile-7
	3a	29.6, CH$_2$	2.34, m	2, 3b	2, 3b, 4a, 4b, 5a, 5b	1	
	3b		1.86, m	2, 3a	2, 3a, 4a, 4b, 5a, 5b	1	
	4a	25.9[e], CH$_2$	2.10, m	4b, 5a, 5b	2, 3a, 3b, 4b, 5a, 5b		
	4b		2.03, m	4a, 5a, 5b	2, 3a, 3b, 4a, 5a, 5b		
	5a	48.5, CH$_2$	3.90, m	4a, 4b, 5b	2, 3a, 3b, 4a, 4b, 5b		Leu-2
	5b		3.64, m	4a, 4b, 5a	2, 3a, 3b, 4a, 4b, 5a		Leu-2
Leu	1	172.1, C					
	2	50.3, CH	4.77, dd (9.9, 4.5)	3a, 3b	3a, 3b, 4	1	Pro-5a, Pro-5b
	3a	42.0, CH$_2$	1.53, m	2, 3b, 4	2, 3b, 4		
	3b		1.50, m	2, 3a, 4	2, 3a, 4		
	4	25.6, CH	1.64, m	3a, 3b, 5, 6	3a, 3b, 5, 6		
	5	23.9[e], CH$_3$	0.95, m	4	2, 4, 6		
	6	21.8, CH$_3$	0.96, m	4	2, 4, 5		
	NH[d]		7.61, d (8.5)	2		N-Me-Leu-1	
N-Me-Leu	1	172.6, C					
	2	55.4, CH	5.21, dd (10.8, 4.5)	3a, 3b	3a, 3b, 4, 5, 6	1	
	3a	37.7, CH$_2$	1.77, m	2, 3b	2, 3b, 4, 5, 6		
	3b		1.49, m	2, 3a	2, 3a, 4, 5, 6		
	4	25.8, CH	1.46, m	5, 6	2, 3a, 3b, 5, 6		
	5	22.1, CH$_3$	0.84, d (6.2)	4	2, 3a, 3b, 4, 6		
	6	23.8[e], CH$_3$	0.93, m	4	2, 3a, 3b, 4, 5		
	7	31.60[e], CH$_3$	3.11, s			2, Val-1	Val-2

Table 1. continued

residue	position	$\delta_C{}^b$	$\delta_H{}^c$ (J in Hz)	COSY	selected TOCSY	selected HMBC (H→C)	selected NOESY
Val	1	175.09^e, C					
	2	56.2, CH	4.60, d (8.8)	3			N-Me-Leu-7
	3	31.62^e, CH	2.07, m	2, 4, 5			
	4	19.8, CH$_3$	0.95, m	3			
	5	19.0, CH$_3$	0.99, d (6.8)	3			
	NH^d		8.18, d (8.0)	2		Ba-1	
Ba	1	176.0, C					
	2	38.4, CH$_2$	2.20, td (7.4, 1.7)	3		1	
	3	20.5, CH$_2$	1.62, m	2, 4		1	
	4	14.0, CH$_3$	0.93, m	3			

^{a}The ^{1}H−^{13}C connectivities were determined using HMQC signals. ^{b}Measured at 125 MHz. ^{c}Measured at 500 MHz. ^{d}Detected in CD$_3$OH. ^{e}These signals are interchangeable.
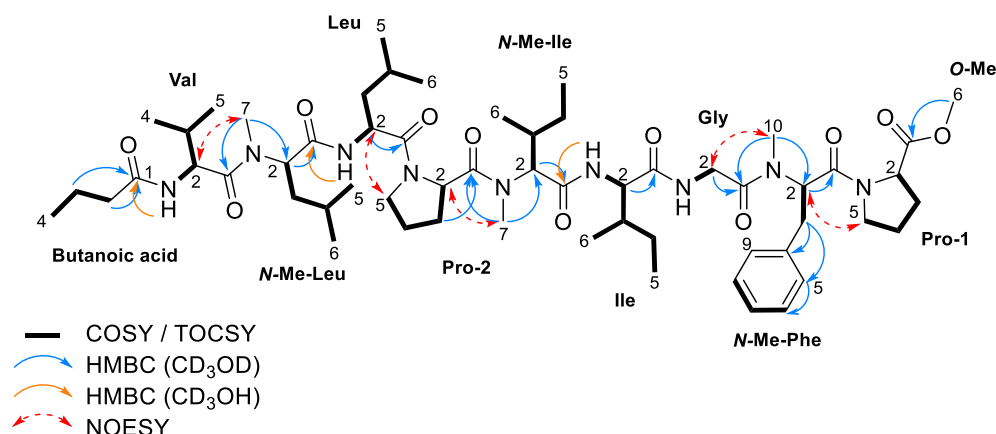

Figure 1. Key correlations from the 2D NMR spectra and the planar structure of amantamide C (**1**).
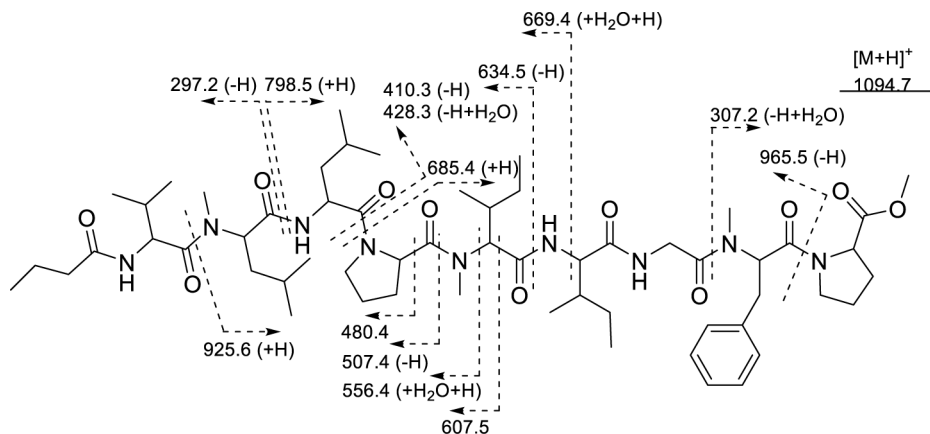

Figure 2. Selected MS/MS fragmentation patterns of amantamide C (**1**).

morphological change, we isolated amantamide C (**1**, 4.7 mg) as an active compound.

The molecular formula of amantamide C (**1**) was determined to be C$_{58}$H$_{95}$N$_9$O$_{11}$ by HR-ESI-MS (m/z 1116.7071, calcd for C$_{58}$H$_{95}$N$_9$O$_{11}$Na [M + Na]$^+$ 1116. 7044). The NMR data are presented in Table 1. The ^{1}H NMR spectrum showed several signals corresponding to α protons of amino acids (δ_H 5.55−3.88 ppm). Three singlet methyl signals observed at δ_H 3.11, 3.05, 3.01 ppm implied the presence of three N-methyl amides, and one singlet methyl signal observed at δ_H 3.71 suggested the existence of one methyl ester group. Additionally, ^{13}C NMR spectrum indicated the presence of ten carbonyl groups (δ_C 176.0, 175.09, 175.08,

174.0, 173.8, 172.6, 172.1, 171.5, 170.3, 170.1). Based on these observations, we hypothesized that **1** was a peptide compound. Further analysis of the COSY, TOCSY, HMQC, HMBC, and NOESY data revealed that **1** was composed of an O-methyl ester group and two prolines: N-Me-phenylalanine, glycine, isoleucine, N-Me-isoleucine, leucine, N-Me-leucine, valine, and butanoic acid (Ba).

Two NOESY correlations, H-5 of Pro-1/H-2 of N-Me-Phe and H-10 of N-Me-Phe/H-2 of Gly, revealed the sequence of Pro-1-N-Me-Phe-Gly. In addition, three HMBC correlations, NH of Ile/C-1 of N-Me-Ile, NH of Leu/C-1 of N-Me-Leu, and NH of Val/C-1 of Ba, and three NOESY correlations, H-7 of N-Me-Ile/H-2 of Pro-2, H-5 of Pro-2/H-2 of Leu, and H-7 of

N-Me-Leu/H-2 of Val, revealed the sequence Ile-*N*-Me-Ile-Pro-Leu-*N*-Me-Leu-Val-Ba. The connections of these three substructures (*O*-Me, Pro-*N*-Me-Phe-Gly, and Ile-*N*-Me-Ile-Pro-Leu-*N*-Me-Leu-Val-Ba) were unequivocally determined based on the molecular formula, as shown in Figure 1. The accuracy of this planar structure was supported by the fragmentation ions detected by tandem mass spectrometry (Figure 2).

The absolute configuration of amantamide C (**1**) was determined by acid hydrolysis, followed by chiral-phase HPLC analysis. *N*-Me-Phe and *N*-Me-*allo*-Ile were found to be in the ᴅ-form, whereas the other residues were in the ʟ-form. Structurally, **1** is a new analog of amantamides (**2** and **3**), in which the *N*-Me-ᴅ-Val residue is replaced with an *N*-Me-*allo*-ᴅ-Ile residue.

We evaluated the growth-inhibitory activity of amantamide C (**1**) against HeLa and HL60 cells using an MTT assay. The cells were treated with varying concentrations of **1** for 72 h. **1** did not show the inhibitory activity against either cell at 10 μM (IC$_{50}$ 91 μM for HeLa cells). Meanwhile, HeLa cells treated with **1** at 50 μM exhibited spindle−like morphological changes after 24 h (Figure S2). Additionally, **1** induced apoptosis-like cell death after 48 h. We also performed a trypan blue dye exclusion assay using HeLa cells (Figure 3). As shown in
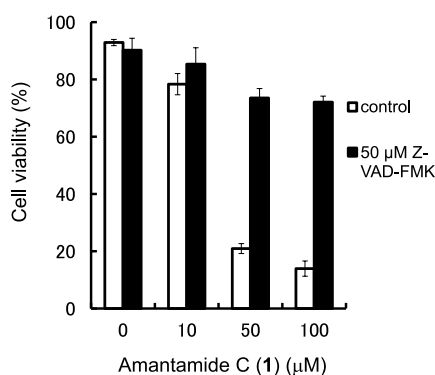

Figure 3. Evaluation of induction of apoptosis by amantamide C (**1**).

Figure 3, **1** decreased cell viability with higher doses, indicating that the cell growth inhibition induced by **1** at 91 μM is derived from its cell-killing activity. In addition, cell death was suppressed in the presence of the pan-caspase inhibitor Z-VAD-FMK. Therefore, **1** was suggested to induce apoptosis in HeLa cells. To explore further biological activities, we assessed the antitrypanosomal activity of **1**. Compound **1** inhibited the growth of *Trypanosoma brucei rhodesiense*, the causative organism of African sleeping sickness, with an IC$_{50}$ value of 2.8 ± 0.2 μM.

■ CONCLUSION

We isolated a new analog of amantamides, amantamide C (**1**), from *Okeania* sp. marine cyanobacteria collected in Japan and established its absolute configuration. In a previous study, amantamide (**2**) was reported as a selective agonist against CXCR7 among 168 GPCR.[6] In addition, it suggested that **2** and amantamide B (**3**) have neuronal excitation activity and/ or potential activity on Ca^{2+} signaling.[8] In this study, we revealed that **1** induced spindle-like morphological changes after 24 h and apoptosis after 48 h against HeLa cells at 50 μM. Spindle-like morphological changes are known to be caused by

ER stress inducers, and one of the main pathways leading to ER stress is by altering Ca^{2+} signaling, which leads to apoptosis.[9] Therefore, our observations in this study support the hypothesis that amantamides (**2** and **3**) affect Ca^{2+} signaling.[8] In our studies on natural products isolated from marine cyanobacteria to date, we have found that marine cyanobacteria produce compounds, such as iezoside[10] and kurahyne,[11] that have activity in Ca^{2+} signaling. This finding indicates that these compounds have an unidentified ecological role in marine ecosystems. Further studies on amantamide-type compounds (**1**−**3**) could provide new insights into the chemical ecosystems of coral reefs mediated by Ca^{2+} signaling. In addition, we found that **1** showed a moderate inhibitory activity against *Trypanosoma brucei rhodesiense* in the first time in amantamide series. As the antitrypanosomal activity of amantamides (**2** and **3**) have not been reported, detailed structure−activity relationship is not revealed.

■ EXPERIMENTAL SECTION

General. Optical rotations were measured with a P-2200 (JASCO). UV spectra were recorded on a UV-1850 (Shimadzu). IR spectra were obtained on a FT/IR-6300 (JASCO). NMR spectra were recorded by a JEOL ECZ-500 spectrometer for ^{1}H NMR (500 MHz) and ^{13}C NMR (125 MHz). ^{1}H NMR chemical shifts (referenced to a residual solvent signal. CHD$_2$OD, CHD$_2$OH: δ 3.31) were assigned based on COSY and HMQC data. Similarly, ^{13}C NMR chemical shifts (referenced to a residual solvent signal. CD$_3$OD, CD$_3$OH: δ 49.0) were assigned using a combination of data from HMQC and HMBC experiments. ESI mass spectra were obtained on JMS-T100LP AccuTOF LC-plus 4G (JEOL). Tandem mass spectra were obtained on timsTOF (Bruker). For reversed-phase open column chromatography, ODS silica gel Cosmosil 75C$_{18}$−OPN (Nacalai Tesque) was used. High performance liquid chromatography (HPLC) analysis was performed using a pump (model PU-4580, JASCO) and a UV detector (model MD-4015, JASCO). Preparative HPLC was performed using a pump (model LC-20AT, Shimadzu) and a UV detector (model SPD-20A, Shimadzu). All chemicals were obtained from a commercial source (Nacalai Tesque).

Sample Collection and Identification. The cyanobacterial sample (810 g, wet weight) was collected on the coast near an eye glasses-shaped rock locally called as "Fugimi" in Tonaki Island in Japan. A cyanobacterial filament was isolated under a microscope and crushed with freezing and thawing. The 16S rRNA genes were PCR-amplified from the isolated DNA using the primer set CYA106F (a cyanobacterial-specific primer) and 16S 1541R (a universal primer). The PCR reaction contained DNA derived from a cyanobacterial filament, 0.5 μL of KOD-Multi and Epi- (Toyobo), 10 μL of each primer (0.5 μM, respectively), 12.5 μL of 2xPCR Buffer for KOD-Multi and Epi-, and H$_2$O for a total volume of 24 μL. The PCR reaction was performed as follows: initial denaturation for 2 min at 94 °C, and amplification by 40 cycles of 10 s at 98 °C and 10 s at 58 °C, and 1 min at 68 °C. PCR products were analyzed on 1% agarose gel in TBE buffer and visualized by ethidium bromide staining. The obtained DNA was sequenced with CYA 106F and 16S 1541R primers. The nucleotide sequence of 16S rRNA genes obtained in this study was used for phylogenetic sequence of the sequences of related cyanobacterial 16S rRNA genes. All sequences were aligned by MEGA (version 11.0.13). The poorly aligned positions and divergent regions were

removed by Gblocks Server (version 0.91b).[12] The obtained 779 nucleotide positions were used for taxonomic analysis. Parameters for Maximum Likelihood (ML) analysis and Bayesian analysis were determined by JModeltest (version 2.1.7).[13,14] The ML analysis was carried out by PhyML (version 20120412),[14] using the TIM+I+G model with a gamma shape parameter of 0.4090, a proportion of invariant sites of 0.4820 and nucleotide frequencies of F (A) = 0.2458, F (C) = 0.2264, F (G) = 0.3063, F (T) = 0.2215. Bootstrap resampling was done on 1000 replicates. The tree produced by ML analysis was displayed by Njplot (version 2.3).[15] The Baysian analysis was performed with MrBayes (version 3.2.6)[16] based on the GTR+I+G model. The Markov chain Monte Carlo process was set at 2 chains, and 1 000 000 generations were carried out. Sampling frequency was set at every 500 generations. The first 100 000 trees were removed as burn-in, and the consensus tree was generated. The Bayesian tree was displayed by Figure tree (version 1.4.2). As a result, the cyanobacterium (accession no. LC815928) was classified into *Okeania* sp.

Extraction and Isolation. The *Okeania* sp. cyanobacterium (810 g, wet weight) was extracted with MeOH (2 L) for 1 week. The extract was filtered, and the residue was extracted with MeOH (1 L) for 1 week again. The extract was filtered, and the combined solution was concentrated. The residue was partitioned with EtOAc (3 × 0.2 L) and water (0.1 L). The combined organic layers were concentrated, and the residue was partitioned between hexane (3 × 0.2 mL) and 90% MeOH (0.3 L). The 90% MeOH layer was concentrated, and the obtained residue (700 mg) was separated by open column chromatography on ODS (7 g) eluted with 40%, 60%, 80%, and 90% aqueous MeOH, MeOH, and CHCl$_3$/MeOH (1/1).

The fraction eluted with 80% aqueous MeOH (170 mg) was purified with HPLC [Cosmosil 5C$_{18}$-MS-II (ϕ 20 mm × 250 mm); solvent MeOH/H$_2$O (80/20); flow rate 5 mL/min; detection UV 215 nm] in 6 batches to yield a fraction containing **1** (19 mg, t_R > 34 min). This fraction was further separated by HPLC [Cosmosil 5C$_{18}$-MS-II (ϕ 20 mm × 250 mm); solvent MeCN/H$_2$O (65/35); flow rate 5 mL/min; detection UV 215 nm] to yield a fraction containing **1** (4.6 mg, t_R > 42 min). The fraction was purified with HPLC [Cosmosil 5C$_{18}$-MS-II (ϕ 20 mm × 250 mm); solvent MeOH/H$_2$O (85/15); flow rate 5 mL/min; detection UV 215 nm] to yield a fraction containing **1** (1.2 mg, t_R = 42 min This fraction induced morphological change in HeLa cells as shown in Figure S1). This fraction was further separated with HPLC [Cosmosil Cholester (ϕ 20 mm × 250 mm); solvent MeCN/H$_2$O (70/30); flow rate 5 mL/min; detection UV 215 nm] to give crude amantamide C (**1**) (0.7 mg, t_R = 39 min). Meanwhile, the fraction eluted with 90% aqueous MeOH was separated by HPLC [Cosmosil 5C$_{18}$-MS-II (ϕ 20 mm × 250 mm); solvent MeOH/H$_2$O (87/13); flow rate 5 mL/min; detection UV 215 nm] in 7 batches to yield a fraction containing **1** (9.2 mg, t_R = 35 min). This fraction was purified with HPLC [Cosmosil Cholester (ϕ 20 mm × 250 mm); solvent MeCN/H$_2$O (70/30); flow rate 5 mL/min; detection UV 215 nm] to give another crude amantamide C (**1**) (5.4 mg, t_R = 39 min). Both crude amantamide C (**1**) fractions were combined and purified by HPLC [Cosmosil PBr (ϕ 20 mm × 250 mm); solvent MeOH; flow rate 5 mL/min; detection UV 215 nm] in 2 batches to give amantamide C (**1**) (4.7 mg, t_R = 47 min).

Amantamide C (1): colorless oil; $[\alpha]^{20}_D$ −11 (*c* 0.24, MeOH); UV (MeOH) λ_{max} (log ε) 205 (4.34) nm; IR (film) 3304, 2961, 2874, 1737, 1683, 1635, 1540, 1497 cm^{-1}; ^{1}H NMR, ^{13}C NMR, COSY, TOCSY, HMBC, and NOESY data, see Table 1; HRESIMS *m/z* 1116.7071 [M + Na]$^+$ (calcd for C$_{58}$H$_{95}$N$_9$O$_{11}$Na, 1116.7044).

Detamination of the Absolute Configuration of Amantamide C (1). Amantamide C (**1**) was hydrolyzed with 6 M HCl (0.1 mL) for 24 h at 110 °C. The crude product was separated by HPLC to give each amino acids [Cosmosil 5C$_{18}$−PAQ (ϕ 4.6 mm × 250 mm); solvent H$_2$O; flow rate 1 mL/min; detection UV 215 nm; retention times (min) of components; Gly (2.7), Pro (3.2), Val (3.5), Ile (4.7), Leu (4.9), *N*-Me-Ile (5.1), *N*-Me-Leu (6.2), *N*-Me-Phe (13.0)].

Each amino acid except for Ile and *N*-Me-Ile was dissolved in H$_2$O (50 μL) and analyzed by chiral-phase HPLC. The retention times were compared to those analytical standards [DAICEL CHIRALPAK (MA+) (ϕ 4.6 mm × 50 mm); flow rate 1 mL/min; detection UV 254 nm; solvent 2.0 mM CuSO$_4$, 2 mM CuSO$_4$/MeCN (90/10)]. With 2.0 mM CuSO$_4$ as a solvent, the retention times of the amino acids in the hydrolyzate matched those of L-Pro (4.4 min; D-Pro, 2.5 min), L-Val (5.4 min; D-Val, 3.1 min.), L-Leu (12.3 min; D-Leu, 6.9), *N*-Me-L-Leu (18.1 min; *N*-Me-D-Leu, 10.4 min). With 2 mM CuSO$_4$/MeCN (90/10) as a solvent, the retention time of the amino acid in the hydrolyzate matched *N*-Me-D-Phe (7.5 min; *N*-Me-L-Phe, 8.4 min).

For Ile and *N*-Me-Ile, we first analyzed them by reverse-phase HPLC analysis and compared the retention times with those of *allo*- and non *allo*-standards, respectively. [Cosmosil PBr (ϕ 4.6 mm × 250 mm); solvent MeCN/H$_2$O (5/95) and 0.1% TFA; flow rate 1 mL/min; detection UV 215 nm]. The retention times of the amino acids in the hydrolyzate matched those of Ile (7.56 min; *allo*-Ile, 7.45) and *N*-Me-*allo*-Ile (7.34 min; *N*-Me-Ile, 7.88 min). Next, they were analyzed by chiral-phase HPLC [DAICEL CHIRALPAK (MA+) (ϕ 4.6 mm × 50 mm); flow rate 1 mL/min; detection UV 254 nm; solvent 2.0 mM CuSO$_4$]. The retention times of the amino acids in the hydrolyzate matched those of L-Ile (14.5 min; D-Ile, 7.3 min), *N*-Me-D-*allo*-Ile (6.8 min; *N*-Me-L-*allo*-Ile, 12.1 min).

Cell Growth Inhibitory Activity Test. The cells were cultured at 37.0 °C with 5% CO$_2$ in DMEM (for HeLa cells, Nissui) or RPMI (for HL60, Nissui) supplemented with 10% heat-inactivated FBS, 100 units/mL penicillin, 100 μg/mL streptomycin, 0.25 μg/mL amphotericin, 300 μg/mL L-glutamine, and 2.25 mg/mL NaHCO$_3$. For growth inhibitory activity test using HeLa cells, cells were seeded at 4 × 10^3 cells/well in 96-well plates (SARSTEDT) and cultured overnight. For cells growth inhibitory activity test using HL60 cells, cells were seeded at 2 × 10^4 cells/well in 96-well plates (SARSTEDT). Various concentrations of compounds were then added, and cells were incubated for 72 h. Cells growth rate was evaluated by the MTT assay.

Trypan Blue Dye Exclusion Assay. Hela cells were seeded at 2 × 10^4 cells/well in 24-well plates (SARSTEDT) and cultured overnight. Then, the plate was incubated for 30 min with or without 50 μM Z-VAD-FMK (PEPTIDE INSTITUTE. INC.), and the cells were treated with various concentrations of amantamide C (**1**) for 48 h. They were stained with 0.4% trypan blue (BIO-RAD) and the cell viability was determined by counting the number of stained (killed) cells.

Evaluation of Antitrypanosomal Activity. *Trypanosoma bruceirhodesiense* (bloodstream form, strain IL-1501)[17] was maintained under a 5% CO_2 atmosphere in HMI-9 medium[18] supplemented with 10% heat-inactivated fetal bovine serum (FBS) at 37 °C. Compound solutions were prepared using DMSO (The maximum concentration was 1%.) and culture medium before the assay. AlamarBlue serial dilution assays[19] were performed to establish the 50% inhibitory concentrations (IC_{50}) based on the protocol described in our previous paper.[20]

ASSOCIATED CONTENT

Supporting Information

The Supporting Information is available free of charge at https://pubs.acs.org/doi/10.1021/acsomega.4c05909.

> NMR spectra of amantamide C (**1**); tandem mass spectra; HPLC chromatograms for determination of the absolute configurations; phylogenetic tree; photographs of **1**-treated cells (PDF)
>
> Raw NMR data files for compounds **1** (ZIP)

AUTHOR INFORMATION

Corresponding Author

Arihiro Iwasaki − *Department of Applied Chemistry, Chuo University, Bunkyo-ku, Tokyo 112-8551, Japan;* orcid.org/0000-0002-3775-5066; Email: aiwasaki686@g.chuo-u.ac.jp

Authors

Natsumi Watanabe − *Department of Applied Chemistry, Chuo University, Bunkyo-ku, Tokyo 112-8551, Japan*

Ghulam Jeelani − *Department of Biomedical Chemistry, Graduate School of Medicine, The University of Tokyo, Bunkyo-ku, Tokyo 113-8654, Japan*

Tomoyoshi Nozaki − *Department of Biomedical Chemistry, Graduate School of Medicine, The University of Tokyo, Bunkyo-ku, Tokyo 113-8654, Japan*

Complete contact information is available at: https://pubs.acs.org/10.1021/acsomega.4c05909

Notes

The authors declare no competing financial interest.

ACKNOWLEDGMENTS

REFERENCES

(1) (a) Williams, P. G.; Yoshida, W. Y.; Moore, R. E.; Paul, V. J. Tasiamide, a cytotoxic peptide from the marine cyanobacterium *Symploca* sp. *J. Nat. Prod.* **2002**, *65*, 1336−1339. (b) Ma, Z.; Song, N.; Li, C.; Zhang, W.; Wang, P.; Li, Y. Total synthesis and stereochemical reassignment of tasiamide. *J. Pept. Sci.* **2008**, *14*, 1139−1147. (c) Williams, P. G.; Yoshida, W. Y.; Moore, R. E.; Paul, V. J. The isolation and structure elucidation of Tasiamide B, a 4-amino-3-hydroxy-5-phenylpentanoic acid containing peptide from the marine Cyanobacterium *Symploca* sp. *J. Nat. Prod.* **2003**, *66*, 1006−1009. (d) Sun, T.; Zhang, W.; Zong, C.; Wang, P.; Li, Y. Total synthesis and stereochemical reassignment of tasiamide B. *J. Pept. Sci.* **2010**, *16*, 364−374. (e) Mevers, E.; Haeckl, F. P.; Boudreau, P. D.; Byrum, T.; Dorrestein, P. C.; Valeriote, F. A.; Gerwick, W. H. Lipopeptides from

the tropical marine cyanobacterium *Symploca* sp. *J. Nat. Prod.* **2014**, *77*, 969−975.

(2) (a) Kwan, J. C.; Eksioglu, E. A.; Liu, C.; Paul, V. J.; Luesch, H. Grassystatins A-C from marine cyanobacteria, potent cathepsin E inhibitors that reduce antigen presentation. *J. Med. Chem.* **2009**, *52*, 5732−5747. (b) Al-Awadhi, F. H.; Law, B. K.; Paul, V. J.; Luesch, H. Grassystatins D-F, Potent Aspartic Protease Inhibitors from Marine Cyanobacteria as Potential Antimetastatic Agents Targeting Invasive Breast Cancer. *J. Nat. Prod.* **2017**, *80*, 2969−2986.

(3) Kanamori, Y.; Iwasaki, A.; Sumimoto, S.; Matsubara, T.; Sato, T.; Suenaga, K. Izenamides A and B, Statine-Containing Depsipeptides, and an Analogue from a Marine Cyanobacterium. *J. Nat. Prod.* **2018**, *81*, 1673−1681.

(4) (a) Iwasaki, A.; Ohno, O.; Sumimoto, S.; Suda, S.; Suenaga, K. Maedamide, a novel chymotrypsin inhibitor from a marine cyanobacterial assemblage of *Lyngbya* sp. *Tetrahedron Lett.* **2014**, *55*, 4126−4128. (b) Takayanagi, A.; Iwasaki, A.; Suenaga, K. Total synthesis and stereochemical reassignment of maedamide. *Tetrahedron Lett.* **2015**, *56*, 4947−4949.

(5) Al-Awadhi, F. H.; Gao, B.; Rezaei, M. A.; Kwan, J. C.; Li, C.; Ye, T.; Paul, V. J.; Luesch, H. Discovery, Synthesis, Pharmacological Profiling, and Biological Characterization of Brintonamides A-E, Novel Dual Protease and GPCR Modulators from a Marine Cyanobacterium. *J. Med. Chem.* **2018**, *61*, 6364−6378.

(6) Liang, X.; Luo, D.; Yan, J. L.; Rezaei, M. A.; Salvador-Reyes, L. A.; Gunasekera, S. P.; Li, C.; Ye, T.; Paul, V. J.; Luesch, H. Discovery of Amantamide, a Selective CXCR7 Agonist from Marine Cyanobacteria. *Org. Lett.* **2019**, *21*, 1622−1626.

(7) Gritsina, G.; Yu, J. CXCR7 as a novel therapeutic target for advanced prostate cancer. *Oncogene* **2023**, *42*, 785−792.

(8) Li, T.; Xi, C.; Yu, Y.; Wang, N.; Wang, X.; Iwasaki, A.; Fang, F.; Ding, L.; Li, S.; Zhang, W.; Yuan, Y.; Wang, T.; Yan, X.; He, S.; Cao, Z.; Naman, C. B. Targeted Discovery of Amantamide B, an Ion Channel Modulating Nonapeptide from a South China Sea *Oscillatoria* Cyanobacterium. *J. Nat. Prod.* **2022**, *85*, 493−500.

(9) (a) Zhou, S.; Yang, J.; Wang, M.; Zheng, D.; Liu, Y. Endoplasmic reticulum stress regulates epithelial-mesenchymal transition in human lens epithelial cells. *Mol. Med. Rep.* **2020**, *21*, 173−180. (b) Geng, F.; Zhu, W.; Anderson, R. A.; Leber, B.; Andrews, D. W. Multiple post-translational modifications regulate E-cadherin transport during apoptosis. *J. Cell Sci.* **2012**, *125* (Pt 11), 2615−2625.

(10) Kurisawa, N.; Iwasaki, A.; Teranuma, K.; Dan, S.; Toyoshima, C.; Hashimoto, M.; Suenaga, K. Structural Determination, Total Synthesis, and Biological Activity of Iezoside, a Highly Potent Ca^{2+}-ATPase Inhibitor from the Marine Cyanobacterium *Leptochromothrix valpauliae*. *J. Am. Chem. Soc.* **2022**, *144*, 11019−11032.

(11) Iwasaki, A.; Ohno, O.; Katsuyama, S.; Morita, M.; Sasazawa, Y.; Dan, S.; Simizu, S.; Yamori, T.; Suenaga, K. Identification of a molecular target of kurahyne, an apoptosis-inducing lipopeptide from marine cyanobacterial assemblages. *Bioorg. Med. Chem. Lett.* **2015**, *25*, 5295−5298.

(12) (a) Talavera, G.; Castresana, J. Improvement of Phylogenies after Removing Divergent and Ambiguously Aligned Blocks from Protein Sequence Alignments. *Syst. Biol.* **2007**, *56*, 564−577. (b) Castresana, J. Selection of Conserved Blocks from Multiple Alignments for Their Use in Phylogenetic Analysis. *Mol. Biol. Evol.* **2000**, *17*, 540−552.

(13) Darriba, D.; Taboada, G. L.; Doallo, R.; Posada, D. jModelTest 2: More Models, New Heuristics and Parallel Computing. *Nat. Methods* **2012**, *9*, 772.

(14) Guindon, S.; Gascuel, O. A Simple, Fast, and Accurate Algorithm to Estimate Large Phylogenies by Maximum Likelihood. *Syst. Biol.* **2003**, *52*, 696−704.

(15) Perriere, G.; Gouy, M. WWW-Query: An On-line Retrieval System for Biological Sequence Banks. *Biochimie* **1996**, *78*, 364−369.

(16) Ronquist, F.; Teslenko, M.; van der Mark, P.; Ayres, D. L.; Darling, A.; Höhna, S.; Larget, B.; Liu, L.; Suchard, M. A.; Huelsenbeck, J. P. MrBayes 3.2: Efficient Bayesian Phylogenetic

Inference and Model Choice Across a Large Model Space. *Syst. Biol.* **2012**, *61*, 539−542.

(17) Kuboki, N.; Inoue, N.; Sakurai, T.; Di Cello, F.; Grab, D. J.; Suzuki, H.; Sugimoto, C.; Igarashi, I. Loop-Mediated Isothermal Amplification for Detection of African Trypanosomes. *J. Clin. Microbiol.* **2003**, *41* (12), 5517−5524.

(18) Räz, B.; Iten, M.; Grether-Bühler, Y.; Kaminsky, R.; Brun, R. The Alamar Blue Assay to Determine Drug Sensitivity of African Trypanosomes (*T. b. rhodesiense* and *T. b. gambiense*) in Vitro. *Acta Trop.* **1997**, *68* (2), 139−147.

(19) Huber, W.; Koella, J. C. A Comparison of Three Methods of Estimating EC_{50} in Studies of Drug Resistance of Malaria Parasites. *Acta Trop.* **1993**, *55*, 257−261.

(20) Umeda, K.; Kurisawa, N.; Jeelani, G.; Nozaki, T.; Suenaga, K.; Iwasaki, A. Isolation and structure determination of a new analog of polycavernosides from marine *Okeania* sp. cyanobacterium. *Beilstein J. Org. Chem.* **2024**, *20*, 645−652.